http://dx.doi.org/10.5012/bkcs.2014.35.6.1727

Ring and Volcano Structures Formed by a Metal Dipyrromethene Complex

Seung Bae Son, Qing Miao,† Ji-Young Shin,† David Dolphin,† and Jae Ryang Hahn*

*Department of Chemistry and Bioactive Material Sciences and Research Institute of Physics and Chemistry, Chonbuk National University, Jeonju 561-756, Korea. *E-mail: jrhahn@jbnu.ac.kr*
†Department of Chemistry, University of British Columbia, 2329 West Mall Vancouver BC Canada V6T 1Z4
Received January 31, 2014, Accepted February 18, 2014

Dichloromethane liquid droplets containing a cobalt dipyrromethene trimer deposited on a graphite surface were found to form coffee ring, toroid ring, or volcano dot structures due to the redistribution of the solute during solvent evaporation. The shapes and size distributions of the ring structures depended on the drying temperature. The shape differences were attributed to the fact that the solvent evaporation rate controlled the self-assembly process that yielded the coffee stain and pinhole structures.

Key Words : Dipyrromethene, AFM, Coffee-ring, Toroid ring, Evaporation

Introduction

The deposition of a molecular solution onto a solid surface sets in motion a complex interplay of interactions that affect the morphology and pattern of the resulting film. Obtaining solid morphologies with unusual shapes is important to the search for new nanoscale material properties and for creating interfaces for emerging applications, such as the production of templates that order adsorbates or growing crystals, the creation of self-healing surfaces, and the preparation of surfaces with tailored properties.[1-3] Among the many nanoscale material shapes yet reported, ring morphologies provide a distinct shape that is challenging to create but that shows promise in nanoreactors[4] or in selective cellular translocation.[5] DNA and other biological molecules can form ring-shaped condensates upon the addition of multivalent ions.[6] Self-assembly approaches to ring formation have been extended to synthetic di-and triblock[7,8] copolymers and amphiphiles.[9] Porphyrins[10-12] and dendrimers[13] form ring structures upon drying on a substrate. A more unusual approach involves the utilization of physical processes, such as drying or confinement at an interface. Organizing and controlling the nanoring formation process on a solid surface poses several challenges.

The evaporation of a liquid droplet to produce a film containing porphyrin derivatives on a solid substrate produces a variety of nano- and meso-scale structures, including rings,[10-12,14,15] volcanos,[12] disks,[16,17] and rods.[18] Although a general understanding of the mechanisms underlying the formation of these structures has yet to be elucidated, it appears that the initial driving force underlying the formation process is provided by the complex interplay between the solvent, substrate, concentration, or evaporation environment. The interplay between evaporation, film rupture instabilities, and hydrodynamics defines a rich class of systems that may become available for nonequilibrium molecular assembly processes rather than for equilibrium molecular self-assembly processes.

Here, we provide an example system in which the self-assembly of a nanostructure on a graphite surface driven by dipyrromethane (DPM) molecules could be controlled by varying the solvent evaporation rate. We found that the shape and size of the DPM-based nanostructures depended on the drying temperature. The DPM derivatives, which can form neutral complexes with a variety of metal ions, have been used as flexible and versatile ligands in supramolecular chemistry applications. For example, bisdipyrromethene metal complexes featuring double helical or triangular structures have been reported.[19-21] We interpreted the temperature dependence of the nanostructure shape and size as indicative of two formation mechanisms, the selection of which appears to be determined by the solvent evaporation rate.

Experimental

A dipyrromethane derivative comprising the cobalt dipyrromethene trimer (CDT; $C_{96}H_{69}Co_3N_{15}$) shown in Figure 1(b) was used as the solute. The synthesis of this complex has been described elsewhere.[22] The structure and purity of each compound was confirmed by ^1H and ^{13}C NMR, MALDI-TOF mass spectrometry, UV-vis spectrophotometry, and FT-IR spectroscopy. The complex is composed of three cobalt dipyrromethene monomers that surround a central cavity. Single crystals of the trimer suitable for X-ray diffraction analysis were obtained. Molecular modeling studies predicted that the outer diameter of the trimer was 2.6 nm and the height was 2.1 nm. Dichloromethane (DCM, 99.9%, Sigma Aldrich) was used as the solvent without further purification. The films were prepared by depositing 1 μL solution droplets (1.0×10^{-5} M) onto a highly oriented pyrrolytic graphite surface (HOPG, MikroMasch, ZYA grade). The droplet was then allowed to dry in air either at room temperature or at 110 °C over 12 h. The droplets spread evenly over the surface to produce a uniform layer of the compound over the entire surface. Atomic force microscopy (AFM) images were acquired in the tapping mode (nano-

Surf, easyScan2) using noncontact mode cantilevers (NCLR-10, nanoworld), or lateral force microscopy (LFM) images were obtained using LFM mode cantilevers (LFMR-10, nanoworld). The concentration and volume of the solution used in the experiment were carefully chosen to ensure that the amount of CDT adsorbed onto the graphite surface was sufficient to provide AFM images that would permit the statistical analysis and characterization of the nanostructures.

Results and Discussion

The direct deposition of a droplet of the CDT dichloromethane solution onto the graphite surface, followed by drying at 110 °C over 12 h, led to the spontaneous formation of two types of CDT assemblies: a ring structure with a closed central region (a "coffee ring"), or a protrusion structure, as shown in the AFM images (Fig. 1). The assemblies were well and randomly dispersed on the surface, and a variety of sizes were observed. A statistical analysis of the structures indicated that 45.8% of the structures were protrusions (Fig. 1(d) and 1(f)) and 54.2% were coffee ring structures (Fig. 1(c) and 1(e)). A cross-sectional cut along each of the two nanostructures (Fig. 1(g) and 1(h)) revealed that the inside of the coffee ring was closed, whereas the protrusion structure assumed a volcano shape. The size dimensions of the structures differed significantly. The average outer and inner diameters of the coffee ring structures were 753 and 536 nm, respectively. The average wall and central height of the coffee ring were 14.6 and 5.8 nm, respectively. The volcano structures were much smaller than the coffee ring structures. The average diameter and height were 312 and 4.1 nm, respectively.

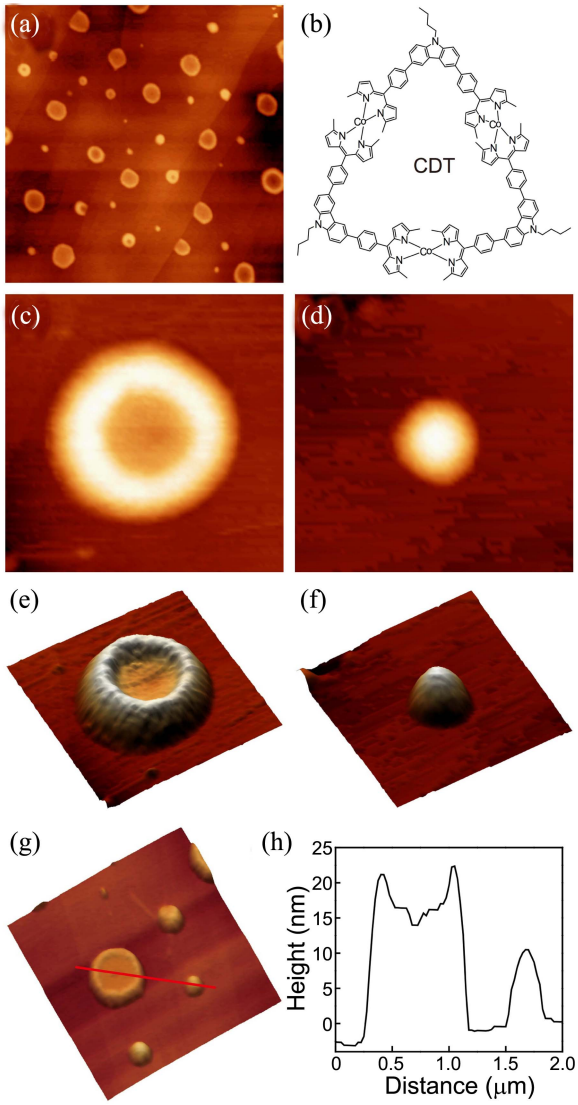

Figure 1. (a) A 3D topographical image, obtained by AFM (tapping mode), of the film left by a 10 μM CDT dichloromethane solution droplet deposited on a graphite surface after drying at 110 °C for 12 h. The scan area is 9 × 9 μm^2. (b) Molecular structure of the cobalt dipyrromethene trimer (CDT, $C_{96}H_{69}Co_3N_{15}$). The magnified images show (c) a coffee ring and (d) a volcano structures. (e) and (f) Corresponding 3D topographical images. (g) The magnified image shows a ring and several volcano structures. The scan area is 3 × 3 μm^2. (h) A cross-sectional cut along the line in image (g).

The central region of the coffee ring structure shown in Figure 1(c) and 1(e) appeared to be filled in the AFM image, unlike the rings produced by porphyrin derivatives, which created toroidal structures. AFM is not an ideal tool for imaging the molecules that were present in the central region. Previously fluorescence images of the ring structures formed from porphyrins were collected to understand the structures of the central areas.[14,15] In the present work LFM imaging was used to characterize the presence of molecules in the central region. LFM measures the friction characteristics of a surface and is useful for characterizing the composition of a surface layer because the measured friction constant will depend on the material. Figure 2 shows LFM and tapping mode AFM (inset) images obtained simultaneously from the same region. The friction force inside the ring was comparable to the forces measured at the ring wall and volcano

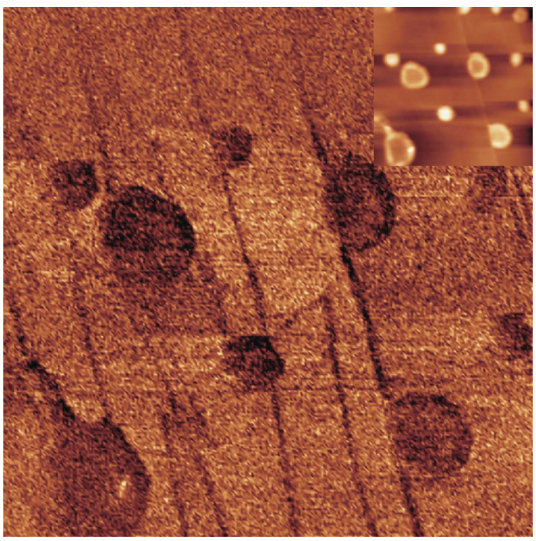

Figure 2. LFM and tapping mode AFM (inset) images obtained simultaneously from the same region, prepared by depositing a 10 μM CDT dichloromethane solution on a graphite surface and drying at 110°C for 12 h. The scan area is 3 × 3 μm^2.

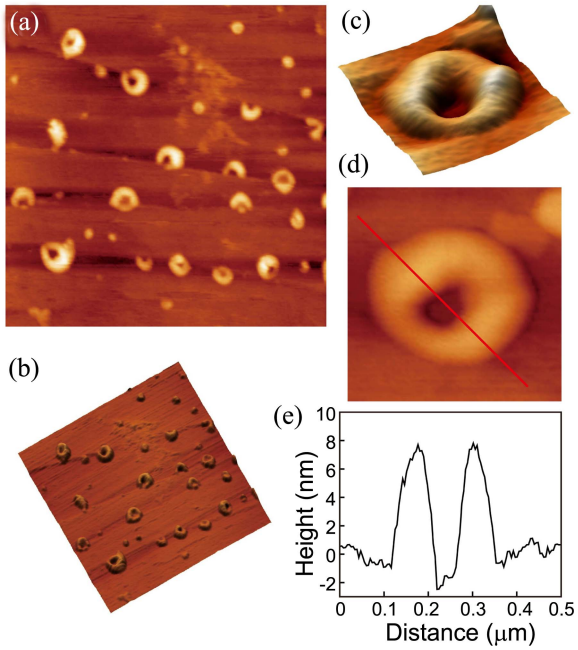

Figure 3. (a) A topographical image, obtained by AFM (tapping mode), of the film left by a 10 μM CDT dichloromethane solution deposited on a HOPG surface and dried at room temperature for 12 h. The scan area is 3 × 3 μm^2. (b) The 3D topographical image of (a). (c) and (d) Magnified 3D and 2D images showing a toroidal ring structure, respectively. The scan area is 0.5 × 0.5 μm^2. (e) A cross-sectional cut along the line shown in image (d).

structures, suggesting that the central region was filled with CDT molecules.

The nanostructure shape changed as the drying temperature decreased. Figures 3(a) and 3(b) show AFM images (2D and 3D) obtained from graphite surfaces dried at room temperature over 12 h after deposition of the CDT dichloromethane solution. Both ring and volcano dot structures were observed and were found to be well dispersed. A statistical analysis of the numbers of each nanostructure revealed that 43.9% were dot and 56.1% were ring nanostructures, similar to the results obtained from the high-temperature drying protocol. The sizes and shapes of the nanostructures, however, differed significantly from the distributions obtained from the high-temperature drying protocol. A cross-sectional cut (Fig. 3(d) and 3(e)) along the ring structure revealed that the central region did not contain atoms, indicating a toroidal ring structure. The height and diameter of the toroidal ring and volcano nanostructures were smaller than the corresponding values obtained using the 110 °C drying protocol.

The size distribution changed as the drying temperature decreased. The sizes of the coffee ring structures varied, with diameters in the range 400–1000 nm and wall heights in the range 7–25 (Figs. 4(a) and 4(b)). By contrast, the toroid rings were relatively monodispersed compared to the coffee rings. The sizes of the toroid rings varied, with outer diameters in the range 100–300 nm (with an average of 200 nm) and heights in the range 2–10 nm (with an average of 5.5 nm) (Fig. 4(c) and 4(d)). The average inner diameter of the toroidal rings was 68 nm and the average thickness of the

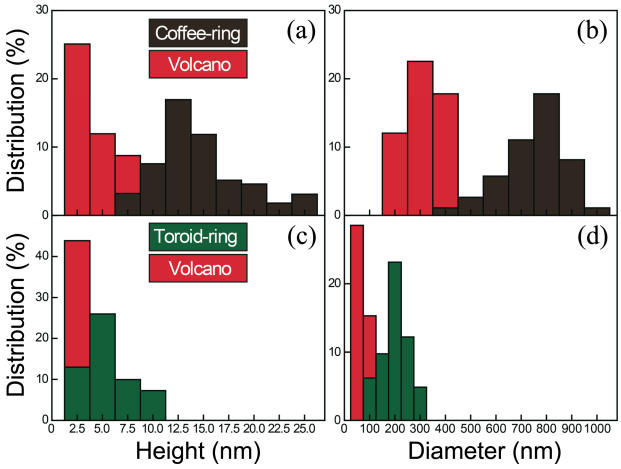

Figure 4. (a) and (b) Statistical distributions of the coffee ring and volcano dot structures as a function of the height and diameter. (c) and (d) Statistical distributions of the toroid ring and volcano dot structures as a function of the height and diameter.

ring wall was 67 nm. The volcano structures formed at room temperature were much smaller, with diameters in the range 50–100 nm (with an average of 68 nm) and heights in the range < 2.5 nm (with an average of 1.8 nm). Interestingly, the sizes of the nanostructures that formed at room temperature were relatively monodisperse compared to the sizes of the nanostructures that formed at higher temperatures.

The process by which ring-like structures form from a liquid droplet depends on the characteristics of the physical dewetting process, the substrate, the solvent, and the solute dynamics, including the rate of evaporation of the liquid, the solubility, and the temperature gradient across the droplet. A coffee stain mechanism was previously suggested as governing the formation of the coffee ring structure shown in Figure 1, as described by Deegan *et al.*[23,24] A coffee ring deposit is left by an evaporating drop with a pinned contact line. Here, the flux of the fluid toward the edge of the droplet leads to the buildup of solute as the droplet evaporates. Both the geometric nature of pinning and the increased evaporation due to the curvature at the droplet's edges contribute to the spatial distribution of the coffee ring. Compensation for the evaporative losses leads to an outward flow of fluid carrying the dispersed material from the interior to the edge of the drop, where the solute is deposited as a solid ring. The solute is not transferred completely, and a fraction of the material remains inside the resulting ring.[25,26]

The appearance (disappearance) of the coffee ring structures at higher (room) temperatures indicated that the temperature of the substrate significantly affected the heat flux from the surface and broke the symmetry that permitted Deegan's solution. At higher temperatures, the heat was readily transferred from the substrate to the pinned edge of the drop, thereby enhancing evaporation near the drop's edges relative to the center. The CDT moved toward the drop's edge and replaced fluid lost to evaporation. Increasing the substrate temperature increased the magnitude of the solute transfer toward the contact line. This model is similar

to the model proposed to explain the results obtained from the inkjet-printed line and the drop cross-sectional analysis,[25] which showed that a higher substrate temperature enhanced the frequency of coffee ring formation.

The toroid rings formed at room temperature were similar to the porphyrin-induced rings. No detectable fluorescence was observed from the insides of the several of the porphyrin rings.[14,15] These results suggested that the centers of the rings were clear, indicating that the mechanism by which the toroid rings formed differed from the coffee stain mechanism. A pinhole mechanism is proposed, in which the formation of holes in the thinning liquid films is proposed to account for the ring formation. In this model, the film thins until reaching a thickness at which holes nucleate. At this equilibrium thickness, film thinning is balanced with the surface wetting. The holes open while the self-assembling particles collect at the growing inner perimeter. The spherical nucleation sites grow in size during evaporation and the solution concentrated increases. The evaporation speed at the edges of a pinhole exceeds the evaporation speed in the bulk of the solution film. The inward flow of solute, which compensates for this loss of liquid, further concentrates the solute at the inner edges of the ring structure. The solution film tends to break due to surface instabilities that induce dewetting at the heterogeneous nucleation sites or to spinodal dewetting. Heterogeneously nucleated holes form during the early stages of evaporation and can grow continuously. As a result, the rings tend to be randomly distributed over the sample and tend to have a range of diameters. The rings formed *via* this mechanism are expected to be small in diameter and monodisperse in size, consistent with our observations. A lower evaporation rate may permit the thin film to reach an equilibrium state.

Our observations of the temperature dependence of the ring deposit structures did not suggest that the surface tension was temperature dependent; however, previous studies of the coffee ring effects warrant a discussion of the surface tension-driven flow, known as the Marangoni effect.[27] These studies showed that the coffee ring effect can be controlled or eliminated by engineering an appropriate type of Marangoni flow. Marangoni flows in an evaporating octane droplet led to the deposition of solute at the center of the droplet, thereby avoiding the formation of a coffee ring at the perimeter. In fact, the formation of more pronounced coffee rings at higher temperatures, as observed here, goes against a model in which the temperature-driven Marangoni flows would be expected to redistribute a larger amount of the CDT solute at the feature's center in the presence of a warm substrate.

Interestingly, the surface concentration (deposited volume after evaporation) obtained at room temperature was more than 11 times the value obtained at higher temperatures. Holding the size and solute concentration of a droplet constant, the total volumes of the nanoring and volcano structures were quantified based on the inner and outer diameters and the heights of the nanorings, or the diameters and heights of the volcano dots. The measurements were collected over a 9 μm × 9 μm region encompassing the drop volume. The density of the deposited volume was calculated to be 1.66×10^6 nm^3 μm^{-2} under high-temperature drying conditions or 1.46×10^5 nm^3 μm^{-2} under room-temperature drying conditions. The liquid droplets were prepared with a given concentration and volume; therefore, the evaporation rate may affect the quantity of solute that remains on the surface.

Conclusion

In conclusion, we showed that a CDT complex formed from a ligand structure that is more flexible and versatile than a porphyrin ligand could enable the formation of coffee ring, volcano dot, and toroid ring structures, depending on the substrate temperature. The distinct morphological dependence on the substrate temperature was attributed to the important effects of the evaporation rate on the formation mechanism. The solvent evaporation rate may determine the ring formation mechanism.

Acknowledgments. This work was supported by grants from the Korean government (NRF, MSIP, 2010-0024254 and 2007-0056095) and by research funds of Chonbuk National University in 2013.

References

1. Lee, K. J.; Pan, F.; Carroll, G. T.; Turro, N. J.; Koberstein, J. T. *Langmuir* **2004**, *20*, 1812.
2. Park, E. J.; Carroll, G. T.; Turro, N. J.; Koberstein, J. T. *Soft Matter* **2009**, *5*, 36.
3. Lancaster, J. R.; Jehani, J.; Carroll, G. T.; Chen, Y.; Turro, N. J.; Koberstein, J. T. *Chem. Mater.* **2008**, *20*, 6583.
4. Djalali, R.; Samson, J.; Matsui, H. *J. Am. Chem. Soc.* **2004**, *126*, 7935.
5. Alexander, L.; Dhaliwal, K.; Simpson, J.; Bradley, M. *Chem. Commun.* **2008**, 3507.
6. Miller, I. C. B.; Keentok, M.; Pereira, G. G.; Williams, D. R. M. *Phys. Rev. E* **2005**, *71*, 31802.
7. Huang, H.; Chung, B.; Jung, J.; Park, H. W.; Chang, T. *Angew. Chem. Int. Ed.* **2009**, *48*, 4594.
8. Pochan, D. J.; Chen, Z.; Cui, H.; Hales, K.; Qi, K.; Wooley, K. L. *Science* **2004**, *306*, 94.
9. Lee, E.; Jeong, Y. H.; Kim, J. K.; Lee, M. *Macromolecules* **2007**, *40*, 8355.
10. Schenning, A. P. H. J.; Benneker, F. B. G.; Geurts, H. P. M.; Liu, X. Y.; Nolte, R. J. M. *J. Am. Chem. Soc.* **1996**, *118*, 8549.
11. Hofkens, J.; Latterini, L.; Oppen, P. van; Faes, H.; Jeuris, K.; Feyter, S. de; Kerimo, J.; Barbara, P. F.; Schryver, F. C. de; Rowan, A. E.; Nolte, R. J. M. *J. Phys. Chem. B* **1997**, *101*, 10588.
12. Latterini, L.; Blossey, R.; J. Hofkens, J.; Vanoppen, P.; Schryver, F. C. de; Rowan, A. E.; Nolte, R. J. M. *Langmuir* **1999**, *15*, 3582.
13. Masuo, S.; Yoshikawa, H.; Asahi, T.; Masuhara, H.; Sato, T.; Jiang, D. L.; Aida, T. *J. Phys. Chem. B* **2001**, *105*, 2885.
14. Lensen, M. C.; Takazawa, K.; Elemans, J. A.; Jeukens, C. R.; Christianen, P. C.; Maan, J. C.; Rowan, A. E.; Nolte, R. J. *Chem. Eur. J.* **2004**, *10*, 831.
15. Jeukens, C. R. L. P. N.; Lensen, M. C.; Wijnen, F. J. P.; Elemans, J. A. A. W.; Christianen, P. C. M.; Rowan, A. E.; Gerritsen, J. W.; Nolte, R. J. M.; Maan, J. C. *Nano Lett.* **2004**, *4*, 1401.
16. Biemans, H. A. M.; Rowan, A. E.; Verhoeven, A.; Vanoppen, P.; Latterini, L.; Foekema, J.; Schenning, A. P. H. J.; Meijer, E. W.; Schryver, F. C. de; Nolte, R. J. M. *J. Am. Chem. Soc.* **1998**, *120*,

11054.
17. Elemans, J. A. A. W.; Lensen, M. C.; Gerritsen, J. W.; Kempen, H. van; Speller, S.; Nolte, R. J. M.; Rowan, A. E. *Adv. Mater.* **2003**, *15*, 2070.
18. Snitka, V.; Rackaitis, M.; Rodaite, R. *Sens. Actuators B* **2005**, *109*, 159.
19. Thompson, A.; Dolphin, D. *J. Org. Chem.* **2000**, *65*, 7870.
20. Zhang, Y.; Thompson, A.; Rettig, S. J.; Dolphin, D. *J. Am. Chem. Soc.* **1998**, *120*, 13537.
21. Chen, Q.; Zhang, Y.; Dolphin, D. *Tetrahedron Lett.* **2002**, *43*, 8413.
22. Miao, Q. Self-Assembly of Oligomeric Dipyrromethene Metal Complexes. Ph.D. Thesis, University of British Columbia, Vancouver, Canada, 2010.
23. Deegan, R. D.; Bakajin, O.; Dupont, T. F.; Huber, G.; Nagl, S. R.; Witten, T. A. *Nature* **1997**, *389*, 827.
24. Deegan, R. D.; Bakajin, O.; Dupont, T. F.; Huber, G.; Nagel, S. R.; Witten, T. A. *Phys. Rev. E* **2000**, *62*, 756.
25. Soltman, D.; Subramanian, V. *Langmuir* **2008**, *24*, 2224.
26. Prasetyo, F. D.; Yudistira, H. T.; Nguyen, V. D.; Byun, D. *J. Micromech. Microeng.* **2013**, *23*, 095028.
27. Hu, H.; Larson, R. G. *J. Phys. Chem. B* **2006**, *110*, 7090.